Eur. Phys. J. B **16**, 81–84 (2000)

THE EUROPEAN PHYSICAL JOURNAL B

EDP Sciences

Spin-wave excitations in finite chain segments of the diluted one-dimensional Heisenberg antiferromagnet $CsMn_{1-x}Mg_xBr_3$

A. Furrer[1,a] and H.-U. Güdel[2]

[1] Laboratory for Neutron Scattering, Eidgenössische Technische Hochschule Zürich and Paul Scherrer Institut, 5232 Villigen PSI, Switzerland
[2] Department of Chemistry, Universität Bern, Freiestrasse 3, 3000 Bern 9, Switzerland

Received 31 December 1999

Abstract. The inelastic neutron scattering technique was employed to study the magnetic excitation spectra in the diluted one-dimensional Heisenberg antiferromagnet $CsMn_{1-x}Mg_xBr_3$ ($x = 0$, 0.05, 0.10, 0.25, 0.50). The spectral response is interpreted in terms of spin-wave excitations in finite chain segments of Mn^{2+} ions, which are found to exist as long as the chain length exceeds twice the wavelength of the spin excitation. This limit determines the crossover into the mesoscopic regime.

PACS. 75.30.Ds Spin waves – 75.40.Gb Dynamic properties (dynamic susceptibility, spin waves, spin diffusion, dynamic scaling, etc.) – 75.50.Ee Antiferromagnetics

Understanding the spectral features of correlated low-dimensional magnetic systems in the presence of nonmagnetic impurities has become a central issue in current studies of high-temperature superconductors [1], spin-ladder systems [2], spin-Peierls compounds [3], etc. Theoretical models have been developed to describe the spectral response for the pure systems [4], giving rise to collective spin excitations, and the same models are usually adapted to the case of low impurity concentrations by renormalization procedures or exact numerical diagonalization [4,5]. There are rigorous theoretical solutions only for the case of a one-dimensional magnetic chain [4]. Upon nonmagnetic dilution the infinite chain is separated into segments of length ℓ which follow a statistical distribution function $p(\ell)$. Whenever ℓ is large compared to the wavelength λ of the collective spin excitation, the spin-wave approach is adequate. On the other hand, when ℓ becomes comparable to λ, the system is in a mesoscopic regime and the spin-wave approach breaks down. The applicability of the spin-wave formalism is therefore dependent on both the impurity concentration and the wavelength of the spin excitation. But where does the crossover to the mesoscopic regime occur?

This question was extensively studied for the random one-dimensional antiferromagnet $(CD_3)_4NMn_{1-x}Cu_xCl_3$ (TMMC:Cu) [6–8]. These experiments yielded the empirical rule $q_c \sim 2\kappa$ where q_c is the critical wave vector of the spin excitation and κ the inverse correlation length, *i.e.*, propagating spin-wave modes can only exist for wavelengths of the order or smaller than the average length of the Mn^{2+} segments. These studies, however, were restricted to low impurity concentrations ($x \leq 0.08$ and $x \leq 0.15$ in Refs. [6,8], respectively), so that the crossover for short wavelength spin excitations could not be probed. The empirical rule $q_c \sim 2\kappa$ was therefore derived from the observation of spin excitations with low wave vectors $q \leq 0.07$ Å^{-1} and consequently low energies which can hardly be resolved from the elastic line (see Fig. 3 in Ref. [8]), so that the crossover from underdamped to overdamped spin waves is often difficult to establish. Moreover, and most surprisingly, no energy renormalisation was found upon dilution (see Fig. 6 in Ref. [7]). We therefore decided to address this question by a systematic neutron spectroscopic study of the magnetic response in the diluted one-dimensional Heisenberg antiferromagnet $CsMn_{1-x}Mg_xBr_3$ over a large impurity range $0 \leq x \leq 0.50$. We analysed the observed energy spectra in terms of a model which allows to look at the contributions of particular segment types individually. We find that the crossover to the mesoscopic regime occurs as soon as the length ℓ of the Mn chain segment becomes smaller than typically twice the wavelength λ of the spin excitation. This empirical rule holds over a wide range of wave vectors q.

The crystal structure of $CsMnBr_3$ is hexagonal and consists of $MnBr_3^-$ chains along the c-direction for which the magnetic Mn^{2+} ions are separated by $R = 3.26$ Å, whereas the interchain distance amounts to 7.91 Å [9]. For the diluted compound $CsMn_{1-x}Mg_xBr_3$ the introduction of nonmagnetic Mg does not change the structural parameters ($CsMgBr_3$ is isostructural to $CsMnBr_3$ and has identical unit cell dimensions), thus the distance R is

[a] e-mail: albert.furrer@psi.ch

constant for any value x. For $CsMnBr_3$ the spin Hamiltonian at temperatures $T > T_N = 8.3$ K is very well-described by a nearest-neighbor Heisenberg model:

$$H = -2J \sum_i \mathbf{S}_i \cdot \mathbf{S}_{i+1}, \tag{1}$$

which yields the spin-wave dispersion

$$\varepsilon(\xi) = 4S|J| \cdot \sin(\pi\xi), \tag{2}$$

where $0 \leq \xi \leq 0.5$ is the reduced wave-vector along the c-direction, $S = \frac{5}{2}$ and $J = (-0.89 \pm 0.01)$ meV [10–12].

Cylindrical single crystals of $CsMn_{1-x}Mg_xBr_3$ ($x = 0$, 0.05, 0.10, 0.25, 0.50) with 7 mm diameter and 14 mm length were grown by the Bridgman technique. The inelastic neutron scattering (INS) experiments were performed at the reactor Saphir at the PSI Villigen with use of a triple-axis spectrometer equipped with a doubly bent C(002) monochromator and a horizontally bent C(002) analyzer. The energy of the scattered neutrons was fixed at 13.7 meV, and a pyrolitic graphite filter was used to suppress higher-order contamination. The single crystals were mounted in a closed-cycle helium refrigerator and oriented so as to place the (101) plane into the scattering plane. All measurements were carried out in the neutron energy-loss configuration at $T = 10$ K for scattering vectors $\mathbf{Q} = (0, 0, 1 + \xi)$ from $\xi = 0$ (zone center) to $\xi = 0.5$ (zone boundary).

In Figure 1 we show the dependence of the energy spectra upon variation of the Mg concentration x for spin excitations at the zone boundary ($\xi = 0.5$). For the pure compound ($x = 0$) the spectral response is perfectly symmetric and can be described by a Gaussian centered at an energy of 8.9 meV according to equation (2). Its linewidth corresponds to the instrumental energy resolution. For low impurity contents ($x = 0.05$ and 0.10) the spectral response is gradually shifted to lower energies, the peak width increases, and the peak shape develops an asymmetry on the low energy side. For high impurity contents ($x = 0.25$ and 0.50) this trend continues, but additional inelastic lines show up which are reminiscent of Mn^{2+} dimer and Mn^{2+} trimer excitations at energies 1.8, 3.6 and 4.3, 6.1 meV, respectively [13].

In Figure 2 we show the dependence of the energy spectra upon the reduced wave-vector ξ for constant Mg concentration ($x = 0.10$). With decreasing ξ the spectral response is shifted to lower energies according to the dispersive character of the spin excitations, and the peak width is increasing which is predominantly an instrumental resolution effect. For $\xi \leq 0.1$ the spin excitations could no longer be separated from the elastic line, *i.e.*, the spectral response has the form of a broad band of quasielastic scattering. Similar features as shown in Figures 1 and 2 were observed for other values of ξ and x.

The spin-wave energies for diluted one-dimensional Heisenberg antiferromagnets were calculated by McGurn and Thorpe using linear spin-wave theory [14]. For a segment with n spins the eigenvalues are given by

$$\varepsilon(\xi_n) = 4S|J| \cdot \sin(\pi\xi_n), \tag{3a}$$

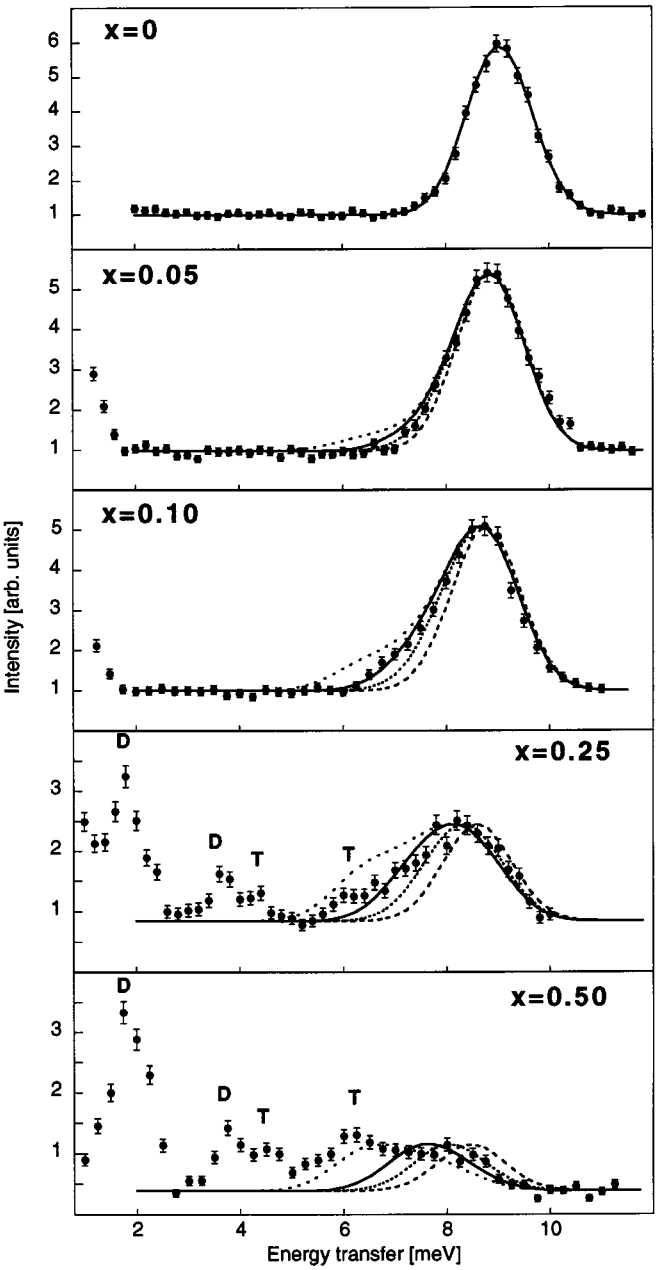

Fig. 1. Energy spectra of neutrons scattered from $CsMn_{1-x}Mg_xBr_3$ at $T = 10$ K and $\mathbf{Q} = (0, 0, 1.5)$. For $x = 0$ the line denotes a Gaussian fit. For $x \neq 0$ the lines are the result of calculations according to equation (5) with $n_1 = 4$ (. . . .), $n_1 = 5$ (—), $n_1 = 6$ (....), and $n_1 = 8$ (- - - -). D and T denote dimer and trimer excitations, respectively [13].

where

$$\xi_n = r/n, \quad \text{with} \quad r = 0, 1, ..., \frac{1}{2}n - 1 \tag{3b}$$

for segments with an even number of spins and

$$\xi_n = \left(r + \frac{1}{2}\right)/n, \quad \text{with} \quad r = 0, 1, ..., \frac{1}{2}(n-3) \tag{3c}$$

for segments with an odd number of spins.

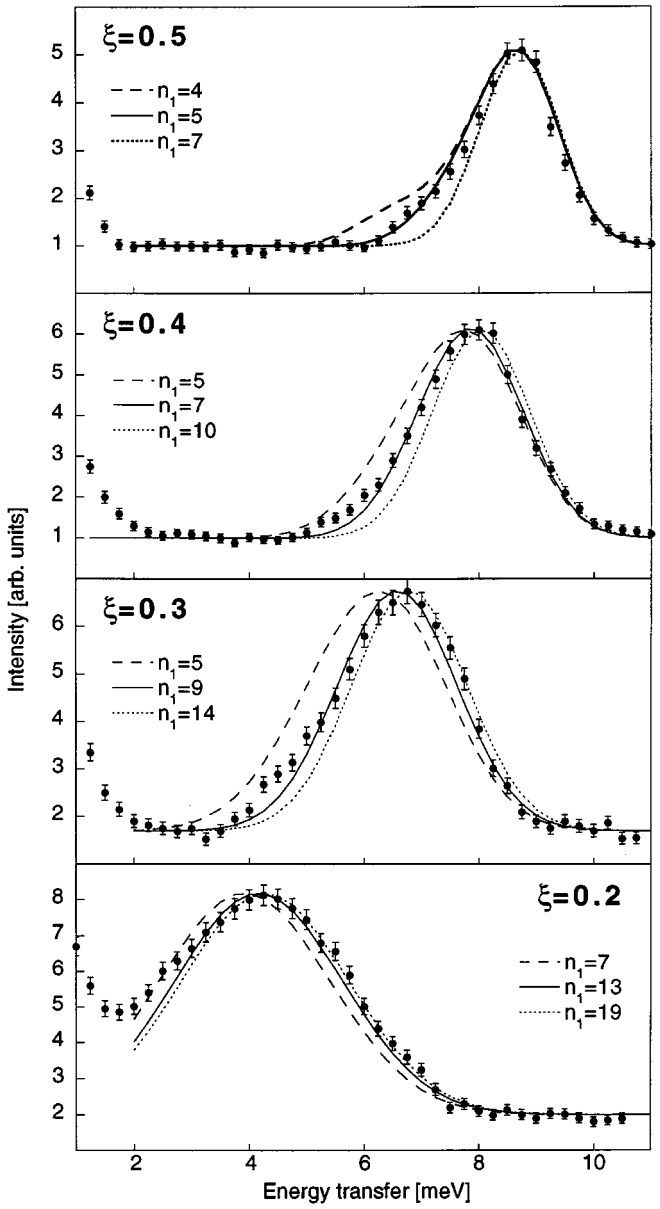

Fig. 2. Energy spectra of neutrons scattered from $CsMn_{0.9}Mg_{0.1}Br_3$ at $T = 10$ K for $\mathbf{Q} = (0, 0, 1 + \xi)$. The lines are the result of calculations as explained in the text.

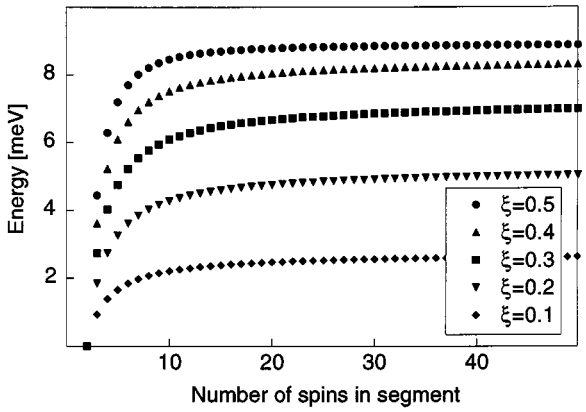

Fig. 3. Calculated spin-wave energies $\varepsilon(\xi)$ *versus* the length of the spin segments for different reduced wave-vectors ξ.

The dispersion relation (3a) is formally the same as for an undiluted spin chain (Eq. (2)), but the finite length of the segments selects certain discrete standing waves that satisfy the boundary conditions. Obviously segments with one and two spins have to be excluded. Based on equations (3) we calculated the wave-vector dependence of the spin-wave energies $\varepsilon(\xi)$ *versus* the length of the segments. For small chain lengths the wave-vector ξ is not always compatible with the discrete values ξ_n given by equations (3); in these cases we set $\xi_n = \xi$, *i.e.*, the spin-wave energy is linearly interpolated from two standing waves (with $\xi_n^{(1)} < \xi < \xi_n^{(2)}$). The results are displayed in Figure 3, which nicely demonstrates the energy renormalization due to the finite chain length.

It was experimentally verified that the nonmagnetic Mg ions enter the chain in a completely random manner [10], thus the lengths of the chain segments thereby created follow a Poisson distribution function [5]

$$p_n(x) = x \cdot \mathrm{e}^{-x \cdot n}. \tag{4}$$

The spectral response for the complete system can then be expressed by the weighted sum over all the segments:

$$S(\xi, \omega, x) \propto \sum_{n=n_1}^{n_2} p_n(x) \left[\left(\exp\left\{ \frac{\varepsilon(\xi_n)}{k_\mathrm{B} T} \right\} - 1 \right)^{-1} + 1 \right] \times \delta\{\hbar\omega - \varepsilon(\xi_n)\}, \tag{5}$$

where $p_n(x)$ and $\varepsilon(\xi_n)$ are defined by equations (3a) and (4), respectively. The summation can be performed numerically, from a lower limit $n_1 = 3$ to an upper limit n_2 where convergence of the wave-vector dependent spin-wave energies is obtained (see Fig. 3). We used $n_2 = 200$ throughout our calculations.

We analyzed the observed energy spectra according to equation (5) which was convoluted with the instrumental resolution function taken from the undiluted analogue. In equation (3a) $4S|J| = 8.9$ meV was kept constant, *i.e.*, no adjustable parameters were introduced (except for an overall intensity scale factor) to describe the spectral response *versus* dilution x as well as reduced wave-vector ξ. The calculations were performed with different values for the lower integration limit n_1 in equation (5). In fact, n_1 sets the limit below which the spin-wave approach is no longer applicable.

Figure 1 shows the results for $\xi = 0.5$ where the collective spin excitations have the shortest wavelength $\lambda = \frac{R}{\xi} = 2 \cdot R$, hence the number of Mn^{2+} ions involved in a single period of the spin wave is $n_s = \frac{\lambda}{R} + 1 = 3$. The energies, linewidths and line shapes of the spectral response for low impurity concentrations ($x = 0.05$ and 0.10) are found to be best described by taking the lower limit in the summation of equation (5) to be $n_1 = 5$ or 6. Smaller and

larger values of n_1 fail to reproduce the observed data. This means that spin-wave excitations at the zone boundary exist in segments whose length ℓ involves at least five or six Mn^{2+} ions, which is roughly twice the wavelength λ of the collective excitations. The situation is more involved for higher impurity concentrations ($x = 0.25$ and 0.50) where the spin-wave-like response at around 8 meV coexists with Mn^{2+} dimer and Mn^{2+} trimer excitations [13], which cannot be reproduced by the spin-wave model (Eq. (3)). Nevertheless, the collective part of the spectral response can be reasonably described by taking $n_1 = 5$ or 6, thereby confirming the results and conclusions obtained for the lower impurity concentrations ($x = 0.05$ and 0.10).

A characteristic feature of introducing impurities into the magnetic chain is the pronounced asymmetry of the spectral response on the low energy side (see Fig. 1). It is interesting to note that similar asymmetric line profiles were observed for TMMC:Cu (see Fig. 12 in Ref. [8]) which could be reproduced by computer simulations. The approach by McGurn and Thorpe [14] used in the present work, however, has the advantage that contributions from particular segment types can be isolated. More specifically, we can clearly assign the observed asymmetry of the peak shape to spin-wave excitations in the smallest chain segments allowed by the empirical rule.

Figure 2 shows the wave-vector dependence of the results obtained for the impurity concentration $x = 0.10$ *versus* the reduced wave-vector ξ. The ξ-dependent wavelength of the spin excitation is defined by $\lambda = \frac{R}{\xi}$, *i.e.*, for the decreasing series of wave-vectors $\xi = 0.5$, 0.4, 0.3, and 0.2 we have $\lambda = 2 \cdot R$, $\frac{5}{2} \cdot R$, $\frac{10}{3} \cdot R$, and $5 \cdot R$, respectively, and the number n_s of Mn^{2+} ions involved in a single period of the spin wave increases from $n_s = 3$ to $n_s \approx 4$, $n_s \approx 5$, and $n_s = 6$, respectively, according to $n_s = \frac{\lambda}{R} + 1$. We find that the best description of the spectral response is obtained by taking the lower limit in the summation of equation (5) to be $n_1 \approx 5$ ($\xi = 0.5$), $n_1 \approx 7$ ($\xi = 0.4$), $n_1 \approx 9$ ($\xi = 0.3$), and $n_1 \approx 13$ ($\xi = 0.2$). Again, there is a remarkable correlation between the numbers n_s and the values n_1 resulting from the interpretation of the experimental data. More specifically, we find the empirical rule $n_1 \approx 2n_s$ which means that spin-wave-like excitations exist in segments of Mn^{2+} ions whose lengths ℓ are at least twice as large as the wavelength λ of the collective spin excitation.

Finite chain segments of Mn^{2+} ions can be produced not only by non-magnetic dilution, but also by renormalization effects in the non-diluted compound $CsMnBr_3$ up to rather high temperatures $T \gg T_N = 8.3$ K [11]. For example, at $T = 39$ K, the spin-wave energy for $CsMnBr_3$ at the zone boundary ($\xi = 0.5$) is shifted downwards from 8.9 meV (at $T = 10$ K) to about 7.8 meV [15], since the correlation length is reduced to approximately 14.3 Å $\approx 4.4 \cdot R$ [16]. This corresponds roughly to the mean length $\langle \ell \rangle = 4.7 \cdot R$ of the chain segments in the compound $CsMn_{0.75}Mg_{0.25}Br_3$ for which the non-magnetic dilution reduces the spin-wave energy at the zone boundary by a similar amount to about 8.0 meV (see Fig. 1). Obviously the model used in the present work is able to account quantitatively for the renormalization effects induced by both non-magnetic dilution and temperature.

In conclusion, we performed INS experiments on $CsMn_{1-x}Mg_xBr_3$ and analyzed the data according to the model of McGurn and Thorpe [14]. If the model is properly modified and restricted with respect to the summation over the spin segments, it is remarkably successful to predict the salient features of spin-wave excitations in diluted one-dimensional antiferromagnets. The renormalization effects upon non-magnetic dilution, *i.e.*, the energy shift, the linewidth as well as the line shape of the spectral response, are quantitatively reproduced without any adjustable parameters. From our analysis an empirical criterion emerged that defines the crossover from the applicability of the spin-wave approach to the mesoscopic regime. In particular, spin-wave-like excitations exist in chain segments provided that their length ℓ exceeds twice the wavelength λ of the spin excitation.

The co-operation of O. Paul in the course of the neutron scattering experiments is gratefully acknowledged. We thank B. Braun and N. Cavadini for interesting discussions as well as the Swiss National Science Foundation for financial support.

References

1. L.P. Regnault, Ph. Bourges, P. Burlet, in *Neutron Scattering in Layered Copper-Oxide Superconductors*, edited by A. Furrer (Kluwer Academic Publishers, Dordrecht, Boston, London, 1998) p. 85.
2. E. Dagotto, T.M. Rice, Science **271**, 618 (1996).
3. L.P. Regnault, Physica B **234-236**, 528 (1997).
4. See, *e.g.*, M. Steiner, J. Villain, C.G. Windsor, Adv. Phys. **25**, 87 (1976).
5. See, *e.g.*, S.W. Lovesey, Solid State Commun. **38**, 953 (1981); S. Haas, Phys. Rev. Lett. **80**, 4052 (1998).
6. J.P. Boucher, C. Dupas, W.J. Fitzgerald, K. Knorr, J.P. Renard, J. Phys. Lett. France **39**, L-86 (1978).
7. Y. Endoh, G. Shirane, R.J. Birgeneau, Y. Ajiro, Phys. Rev. B **19**, 1476 (1979).
8. Y. Endoh, I.U. Heilmann, R.J. Birgeneau, G. Shirane, A.R. McGurn, M.F. Thorpe, Phys. Rev. B **23**, 4582 (1981).
9. J. Goodyear, D.J. Kennedy, Acta Cryst. B **28**, 1640 (1972).
10. U. Falk, A. Furrer, H.U. Güdel, J.K. Kjems, Phys. Rev. B **35**, 4888, 4893 (1987).
11. M. Eibschütz, R.C. Sherwood, F.S.L. Hsu, D.E. Cox, in *Magnetism and Magnetic Materials, AIP Conf. Proc. No. 10*, edited by C.D. Graham, J.J. Rhyne (AIP, New York, 1972), p. 684.
12. M.F. Collins, B.D. Gaulin, J. Appl. Phys. **55**, 1869 (1984).
13. U. Falk, A. Furrer, J.K. Kjems, H.U. Güdel, Phys. Rev. Lett. **52**, 1336 (1984); U. Falk, A. Furrer, H.U. Güdel, J.K. Kjems, Phys. Rev. Lett. **56**, 1956 (1986).
14. A.R. McGurn, M.F. Thorpe, J. Phys. C: Solid State Phys. **16**, 1255 (1983).
15. W. Breitling, W. Lehmann, R. Weber, N. Lehner, V. Wagner, J. Magn. Magn. Mater. **6**, 113 (1977).
16. W.J. Fitzgerald, D. Visser, K.R.A. Ziebeck, J. Phys. C: Solid State Phys. **15**, 795 (1982).